Effects of amine organic groups as lattice in ZSM-5 on the hydrolysis of dimethyl ether

Jittima Meeprasert[a], Siriporn Jungsuttiwong[b], Thanh N. Truong[c],
Supawadee Namuangruk[a],*

[a] National Nanotechnology Center, National Science and Technology Development Agency, Klong Luang, Pathumthani 12120, Thailand
[b] Center for Organic Electronic and Alternative Energy, Department of Chemistry and Center of Excellence for Innovation in Chemistry, Faculty of Science,
Ubon Ratchathani University, Ubon Ratchathani 34190, Thailand
[c] Henry Eyring Center for Theoretical Chemistry, Chemistry Department, University of Utah, 315 S 1400 E, Room 2020, Salt Lake City, UT 84112, USA
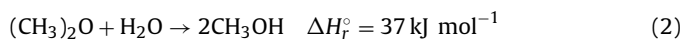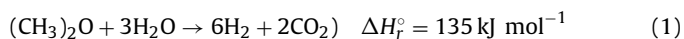
ARTICLE INFO

ABSTRACT

The effects of doping amine to ZSM-5 on its catalytic activity for hydrolysis of dimethyl ether (DME) have been studied theoretically using Density Functional Theory with the embedded cluster ONIOM(M06/6-31G(d,p):UFF) model. Doping by amine to ZSM-5 yields two new active centers, namely the protonated $Z[NH_2]$ and non-protonated $Z[NH]$ amine sites in addition to the normal Brønsted acid $Z[OH]$ site. The reaction has two possible stepwise and concerted channels. The stepwise channel consists of two elementary steps; (i) the demethylation followed by (ii) the hydrolysis while the concerted channel involves in the demethylation and hydrolysis in a single step. We found that the reaction favors to proceed via the concerted channel at all three active centers. The results predict that the $Z[OH]$ shows the best catalytic performance for the studied reaction. The $Z[NH_2]$ is not catalytically active due to the activation barriers are extremely high for both stepwise and concerted pathways. The demethylation step is energetically favorable over the $Z[NH]$ site, however, the product methylamonium surface intermediate is too stable to be further converted to methanol.

© 2013 Elsevier Inc. All rights reserved.

1. Introduction

Hydrogen is becoming an important alternative clean energy source. It can be produced by steam reforming of various oxygenated hydrocarbons such as methanol, ethanol, and dimethyl ether (DME). Among these compounds, DME has a great potential for production of hydrogen due to it is harmless while still provides a high hydrogen to carbon ratio [1,2]. The overall reaction for the steam reforming of DME is given in (Eq. (1)) comprises of two moderately endothermic reactions in sequence: DME hydrolysis to methanol (Eq. (2)) followed by methanol reforming to hydrogen and carbon dioxide (Eq. (3)) [2–4].

$$(CH_3)_2O + 3H_2O \rightarrow 6H_2 + 2CO_2) \quad \Delta H_r^\circ = 135\,kJ\,mol^{-1} \tag{1}$$

$$(CH_3)_2O + H_2O \rightarrow 2CH_3OH \quad \Delta H_r^\circ = 37\,kJ\,mol^{-1} \tag{2}$$

$$CH_3OH + H_2O \rightarrow 3H_2 + CO_2 \quad \Delta H_r^\circ = 49\,kJ\,mol^{-1} \tag{3}$$

It is known that the first step, the DME hydrolysis to methanol (Eq. (2)) is the rate-determining step of the overall reforming process [5]. Lowering the activation energy for this step would be the goal for enhancing the hydrogen production level of this process. This can be done by using a heterogeneous catalyst such as zeolites. ZSM-5 zeolite has been reported by Semelsberger et al. [6] to be the most active catalyst for DME hydrolysis. Recently, we have investigated the reaction mechanisms of the DME hydrolysis over H-ZSM-5 in a combined theoretical and experimental study [4]. The reaction mechanism consists of competitive stepwise and concerted pathways. The dominant pathway was found to be the concerted one in which the demethylation and hydrolysis of DME to methanol occurred in a single step. The minor stepwise pathway yields the alkoxides as stable intermediates between the demethylation and hydrolysis steps. There have also been a number of prior theoretical studies on similar processes on zeolites [7–9].

Zeolite Organic groups as Lattice (ZOL) materials was first synthesized by Yamamoto et al. [10] and confirmed by proton mobility measurement [11] where methylene groups ($-CH_2-$) are incorporated into the zeolite framework by superseding lattice oxygen atom. Since then other organic groups such as amine ($-NH-$) have been successfully incorporated into zeolite framework. In fact, amine ZOL denoted as ZOL-N has been found experimentally

[12,13] and theoretically [14–16] to be rather stable and have strong Lewis base character. ZOL-N material was found to be a very active catalyst for the Knoevenagel reaction [13] typically activated by basic catalysts. ZOL-N was reported to have a lower acid strength compared to the undoped-zeolite [17]. However, several computational studies suggested that ZOL-N can act as a bi-functional acid/base catalyst due to the presence of both basic NH and acidic OH sites in the same region [18–20] and thus ZOL-N material potentially can catalyze a wider range of reactions.

This study we performed systematic computational study of the effect of ZOL-N on the catalytic activity of the DME reforming process by ZSM-5 since the alkoxide species is well-known as a stable surface intermediate upon adsorption of olefins, dehydration of alcohols and including ethers on acidic catalysts [21]. It has been reported that unsaturated hydrocarbons can be protonated at the C–C double bond by Brønsted acid. The other carbon from the double bond subsequently binds to the bridging oxygen sitting between Si and Al (Lewis basic site) forming the alkoxide species. Such oxygen could be replaced by an NH group in ZOL-N zeolite that can be converted into an alkylammonium as reaction intermediate instead of alkoxide. Furthermore, previous theoretical calculations indicated that ZOL-N is capable of lowering activation barriers of the alkylammonium formation as compared to that for the alkoxide species [19,20,22]. It should be noted that both of alkylammonium and alkoxide are only intermediates and thus whether ZOL-N can enhance the performance of the overall DME conversion, complete energy profiles along the two possible reaction pathways must be calculated. Such calculation has not been done previously and will be done in this study.

In this work, we report a theoretical study on the effects of amine organic as lattice groups in ZSM-5 in the hydrolysis of DME. The results will help us to understand the possibility of using the amine ZOL in ZSM-5 for further hydrogen production process by DME steam reforming. Furthermore, the information would provide further understanding on the nature of ZOL as catalytic active sites and thus improving its use in functional design of catalyst for a given reaction.

2. Models and methods

For this study, the ONIOM embedded cluster method [23] was employed. The ONIOM method, which has been successfully used in previous studies [4,24–27], was selected to treat the reactive region of zeolite. The active center was presented by a 128T cluster model, containing 127 Si and one Al tetrahedral atoms, taken from the lattice structure of ZSM-5 zeolite [28] (see Fig. 1a). The dangling bonds from cutting the Si–O bonds were capped by hydrogen atoms with the Si–H bond distance of 1.47 Å in the crystallographic Si–O directions and were constrained to avoid unrealistic distortions of the model during geometry optimizations. The 128T cluster was subdivided into two layers. The inner layer consists of twelve tetrahedral atoms (12T) which are located at the cross section of the straight and zigzag channels and are considered as the active region that allows the guest molecules to react with the acidic proton, while the outer layer is the rest of the model.

For ZOL-N sites, it is known experimentally that nitridation of H-ZSM-5 mainly occurred at Brønsted acid sites [29–31]. Thus, to represent ZOL-N sites in ZSM-5, a selected bridging oxygen atom connecting to the Al atom was substituted by either: (i) a non-protonated amine group ($\equiv$Si–OH–Al–NH–Si$\equiv$), denoted as Z[NH] (note Z[NH] center consists of both OH and NH sites at the same Al tetrahedron) or (ii) a protonated amine group ($\equiv$Si–O–Al–NH$_2$–Si$\equiv$), denoted as Z[NH$_2$]. The geometries of both groups were constructed based on available experimental data [12,13]. The charge and spin multiplicity for all structures are 0

Table 1
Calculated deprotonation energies (E_{DP}), adsorption energies of DME and methanol (MeOH) in the Z[NH$_2$], Z[NH] and Z[OH]. Energies are in kJ/mol.

Models	E_{DP}	MeOH adsorption	DME adsorption
Z[NH$_2$]	1381	−99	−102
Z[NH]	1303	−113	−119
Z[OH]	1293	−114	−118
	1187–1329[a]	−110[e]	−123[e]
	1147–1154[b]	−115 ± 5[f]	−82.4[g]
	1234[c]		−95.5[h]
	1284–1369[d]		

[a] Experimental value from IR spectroscopy [34].
[b] Experimental value from IR spectroscopy [35].
[c] Theoretical value from QM-Pot scheme [36].
[d] Theoretical value from ONIOM(B3LYP/6-311+G**:MNDO), 46-54T atoms [37].
[e] Theoretical value from optimization by 12T/128T ONIOM2 (B3LYP/6-31G(d,p)//UFF) and single point by 34T/128T embedded-ONIOM2 (M06-2X/6-311G(2df,2p)//UFF) [9].
[f] Experimental value from calorimetric study [44].
[g] Experimental value from FT-IR spectroscopy [45].
[h] Theoretical value from ONIOM(B3LYP/DZVP2:HF/6-31G), 31T model [46].

and 1, respectively. The optimized geometries of the models are shown in Fig. 1b and c for the Z[NH] and Z[NH$_2$] site, respectively.

The 12T inner layer represented with ball and stick model in Fig. 1 including the reacting molecule were treated with the M06/6-31G(d,p) level of density functional theory. The rest of the model was treated with the universal force field (UFF) to represent the confinement effect of the zeolite pore structure and to reduce the computational demand. The combination between M06 and UFF in ONIOM method has been successfully used for the study of the reaction mechanisms in zeolites [32].

All calculations were performed by the Gaussian09 program [33]. The TS optimization was used to locate the transition state structures. In additions, the vibrational spectra were performed at the same level of theory to confirm whether the structure is the real saddle point for the studied reaction. The zero-point energy correction (ZPE) was neglected due to we focused on the relative energy and reaction mechanism and thus it would not change the conclusion.

3. Results and discussion

3.1. Models of active centers

ZOL-N ZSM-5 zeolite has three possible active centers, namely the protonated Z[NH$_2$] and non-protonated Z[NH] amine centers and the un-substituted Brønsted acid Z[OH] sites. The optimized structures of these centers are shown in Fig. 1. In consistence with previous reports [15,17], we found that substitution of a basic oxygen atom by amine group at the active site of zeolite have a small effect on the zeolite structures. The Si1–O1 and Al–O1 bond lengths are slightly decreased while the Si2–N and Al–N bond lengths are slightly elongated. These cause the smaller bond angle in the Si2–N–Al in amine-doped ZSM-5 as compared that of Si2–O2–Al in ZSM-5. In addition, the O–H bond distance of the Z[NH] center (O1-Ho, 0.969 Å) is almost equal to that of the Z[OH] center (O1-Hz, 0.967 Å). For the Z[NH$_2$] model, both N-H bond lengths (N-Hn1 and N-Hn2) are longer than those of the Z[NH] center.

The acid strength of a Brønsted acid site in zeolite can be quantified by its deprotonation energy (E_{DP}). Table 1 lists the experimental and calculated deprotonation energies. Our calculated E_{DP} of 1293 kJ/mol for the Z[OH] center is in the range of the experimental [34,35] and previous theoretical [36,37] values for H-ZSM-5. For the Z[NH] and Z[NH$_2$], the calculated E_{DP} values are 1303 and 1381 kJ/mol, respectively, indicating that acidity of zeolite models decreases in the order: Z[OH] > Z[NH] > Z[NH$_2$]. To verify this prediction, the adsorptions of probe molecules (DME and methanol)
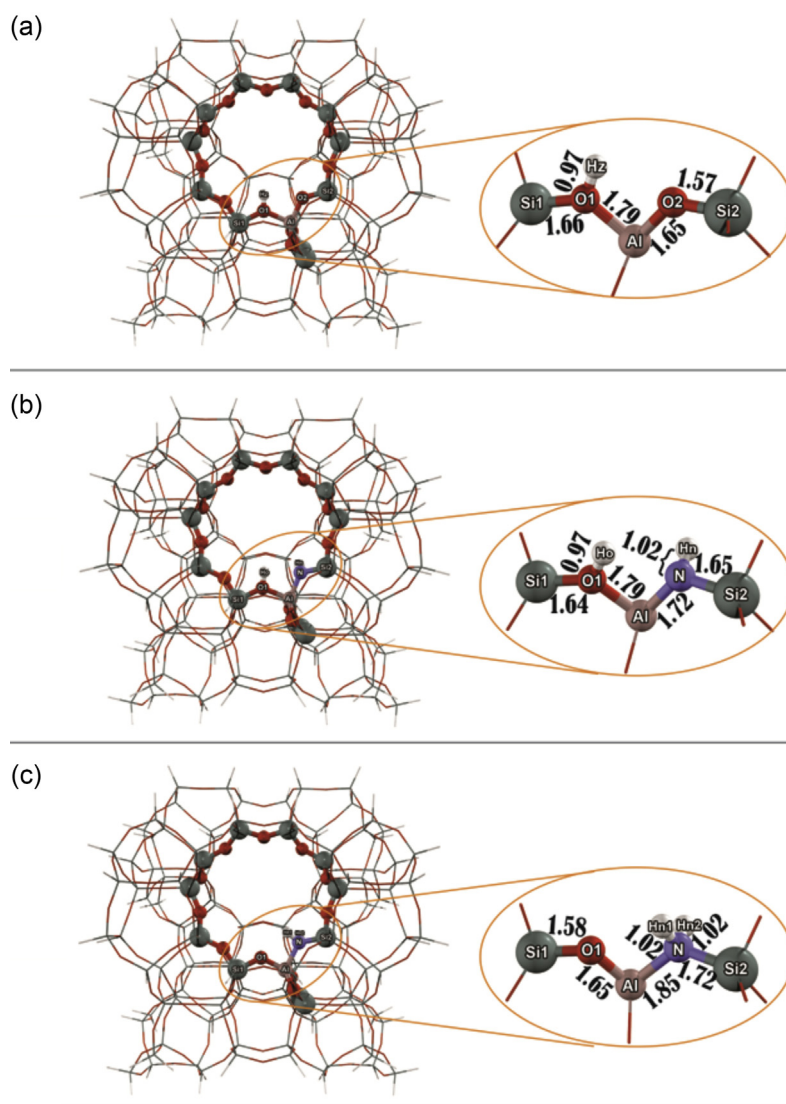
Fig. 1. The optimized geometries for the 128T cluster for the (a) Z[OH], (b) Z[NH]) and (c) Z[NH$_2$]. The quantum region is represented by the balls and sticks, while the UFF region is drawn as lines. Distances are in Å.

on these three centers were calculated and discussed in the next section.

3.2. Adsorptions of methanol and DME

Methanol is a product of the DME hydrolysis over H-ZSM-5. It was known that methanol adsorbed on a Brønsted acid site with either an end-on or side-on mode [4,38–43]. The side-on adsorption mode has one hydrogen bond between the OH group of methanol and the Brønsted acid site. The end-on adsorption mode has two hydrogen bonds and thus is much more stable. For this reason, in this work, we compared the adsorption structures of methanol on the Z[OH], Z[NH] or Z[NH$_2$] active site only in the end-on adsorption mode as shown in Fig. 2a. The adsorbed methanol strongly interacts with the three centers via two hydrogen bonds (one between the oxygen atom of methanol (Om) and the zeolitic proton (Hz); and another between the methanol proton (Hm) and the basic site of zeolite). These hydrogen bond distances are in the range of 1.88-2.04 Å. The acidic O—Hz bonds of the Z[OH] and Z[NH] models are elongated by 0.06 Å while the N—H bond of the Z[NH$_2$] is slightly elongated by 0.02 Å upon adsorption. This indicates that acidity of the Z[NH$_2$] site is the lowest, which is consistent with the

calculated E_{DP} values above and previous studies [15,30]. The calculated adsorption energies of methanol on the three centers are as −99, −114 and −113 kJ/mol for the Z[NH$_2$], Z[NH] and Z[OH], respectively. The calculated adsorption energies of methanol on the Z[OH] site (−113 kJ/mol) is in good agreement with the experimental value of −115 kJ/mol and thus supporting the level of theory employed here [44]. The trend of adsorption energies corresponds to the acidity of zeolite active sites and confirms the prediction above based on their deprotonation energies.

The optimized structures of DME adsorbed on the Z[NH$_2$], Z[NH] and Z[OH] centers are illustrated in Fig. 2b. Similar to the methanol adsorption, DME prefers the end-on adsorption mode. DME adsorbs via hydrogen bond between the oxygen Od of DME and the Hz of ZSM-5 as suggested by FT-IR spectroscopic data [45] and previous theoretical studies [4,9,46]. The structural parameters of the adsorption complexes are only slightly different from those of an isolated molecule. The calculated DME adsorption energies are −102, −119, −118 kJ/mol for the Z[NH$_2$], Z[NH] and Z[OH] centers, respectively. Our calculated DME adsorption energy (−118 kJ/mol) at the Z[OH] center is slightly smaller than the previous theoretical study (−123 kJ/mol) [9]. In addition, the different calculated adsorption energy between DME and MeOH of about 5 kJ/mol is
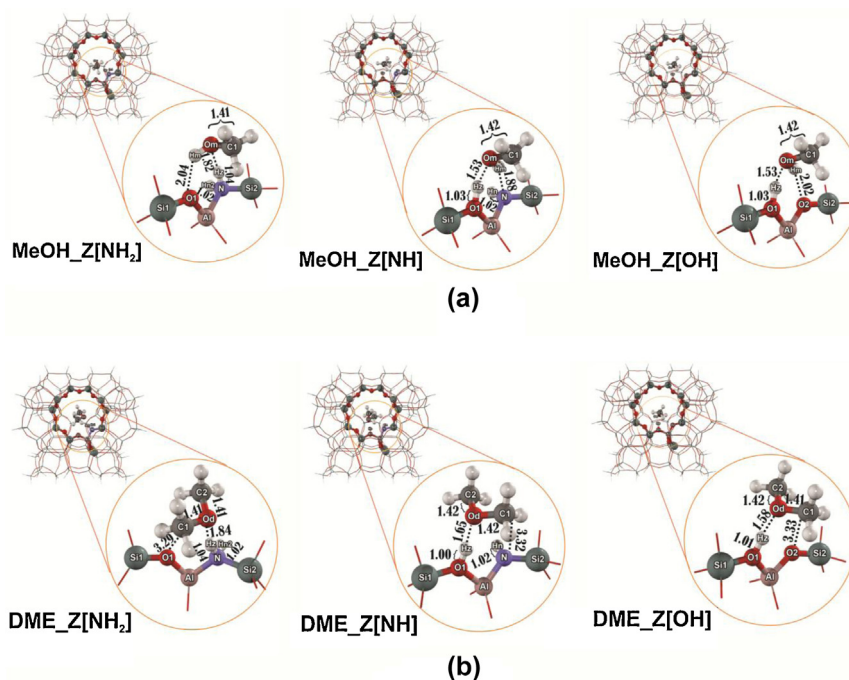
Fig. 2. Optimized structures of (a) methanol (MeOH) and (b) DME adsorptions on the Z[NH$_2$], Z[NH] and Z[OH]. Distances are in Å.

comparable to the different of heats of adsorption of diethylether (DEE) (−135 kJ/mol) and ethanol (EtOH) in H-ZSM-5 (−130 kJ/mol) reported by Lee and Gorte [44].

3.3. Reaction mechanisms of the DME hydrolysis

Hydrolysis of DME over the Z[NH$_2$], Z[NH], and Z[OH] centers can proceed via two possible channels, namely the concerted and stepwise channels. The main difference between the two channels is that the stepwise channel yields the methoxide intermediate while the other channel produces two resultant methanol molecules without forming of any surface intermediate. Our previous results [4] showed that at low temperature DME prefers to be hydrolyzed to methanol over Z[OH] through the concerted mechanism, the stepwise mechanism required activation energy of 60 kJ/mol higher than the concerted one. The effects of doping ZSM-5 by amine on the mechanism of this reaction are discussed below.

A. Concerted channel: This channel consists of two steps, (1) the DME hydrolysis followed by (2) the proton shuttle reactions which are illustrated in Figs. 3 and 4, respectively.

(A1) The DME hydrolysis step: Fig. 3 illustrates that adsorbed DME is hydrolyzed to yield two methanol molecules. This step starts with DME molecule diffuses into the pore of ZSM-5 and adsorbs on the Brønsted acid site to form the DME adsorption complex (DME_Ads). Fig. 3 shows the optimized structures and Tables S1, S2, and S3 (see supporting information) list the selected parameters for all complexes in the Z[NH$_2$], Z[NH] and Z[OH] centers, respectively. The details of DME_adsorption are described earlier in the Section 2.2. Subsequently, water molecule is weakly co-adsorbed next to the adsorbed DME by interacting with the oxygen (or nitrogen for the Z[NH]) basic site of zeolite (denoted as DME_H$_2$O_Ads in Fig. 3). The adsorption energies for all co-adsorbed complexes are −163, −157 and −179 kJ/mol for the Z[OH], Z[NH] and Z[NH$_2$], respectively. These complexes proceed to form two methanol molecules via the transition state (TS). At the TS structure, the C1—O3 bond of the adsorbed DME is elongated by about 0.4–0.5 Å, while the methyl group is moving toward the water molecule

(C1–Ow = 1.81–2.06 Å). Simultaneously, the acidic proton of zeolite (Hz, Ho and Hn1) is transferred to the oxygen atom of DME (O3) while the proton of water molecule is transferring to the basic site of zeolite. The calculated Hw–O2, Hw–N and Hw–O1 distances are 1.95, 1.69, and 3.31 Å, respectively. All TS structures were confirmed by normal mode analyses showing one imaginary frequency for each structure at 413i, 455i and 392i cm^{-1} for the Z[OH], Z[NH] and Z[NH$_2$], respectively, corresponding to the motions of atoms described above.

Subsequently, the two product methanol molecules are co-adsorbed on the zeolite (denoted as Prd_2a) with the adsorption energies of −171, −233 and −96 kJ/mol, for the Z[OH], Z[NH] and Z[NH$_2$], respectively. One methanol molecule desorbs from the active center requiring an energy of 92, 73 or 77 kJ/mol for those at the Z[OH], Z[NH] or Z[NH$_2$] site, respectively, and leaves the other methanol on the Brønsted acid (denoted Prd_2b), see Fig. 4. Note that Brønsted acid protons of Prd_2b complexes are sitting at the O2, N and O1 for the Z[OH], Z[NH] and Z[NH$_2$] centers, respectively.

(A2) The proton shuttle step: To regenerate the active center a proton hopping step is required from the methanol adsorbed complexes Prd_2b (see Fig. 4). It can take place via transition states (denoted as TS_Hshuttle) to form different method adsorbed complexes (denoted as Prd_1e). This requires an activation energy of 5, 67, 3 kJ/mol for the Z[OH], Z[NH] and Z[NH$_2$], respectively. The role of the adsorbed methanol here is to assist the shuttling of proton to regenerate the Brønsted acid site resulting in low activation barriers for such steps. Finally, the adsorbed methanol (Prd_1e) in the end-on mode (described in Section 3.2) can be desorbed from the acid site with the desorption energy of 114, 113 and 99 kJ/mol for the Z[OH], Z[NH], and Z[NH$_2$], respectively.

Fig. 5 shows energy profiles for the DME hydrolysis over the three active centers along the concerted channel. The intrinsic activation energies of the DME hydrolysis step are 125, 142 and 242 kJ/mol and those of the proton shuttle are 5, 67 and 3 kJ/mol for the Z[OH], Z[NH] and Z[NH$_2$], respectively. It is clear that the first step is the rate-determining step for the concerted channel. These results indicate that formations of methanol molecules by
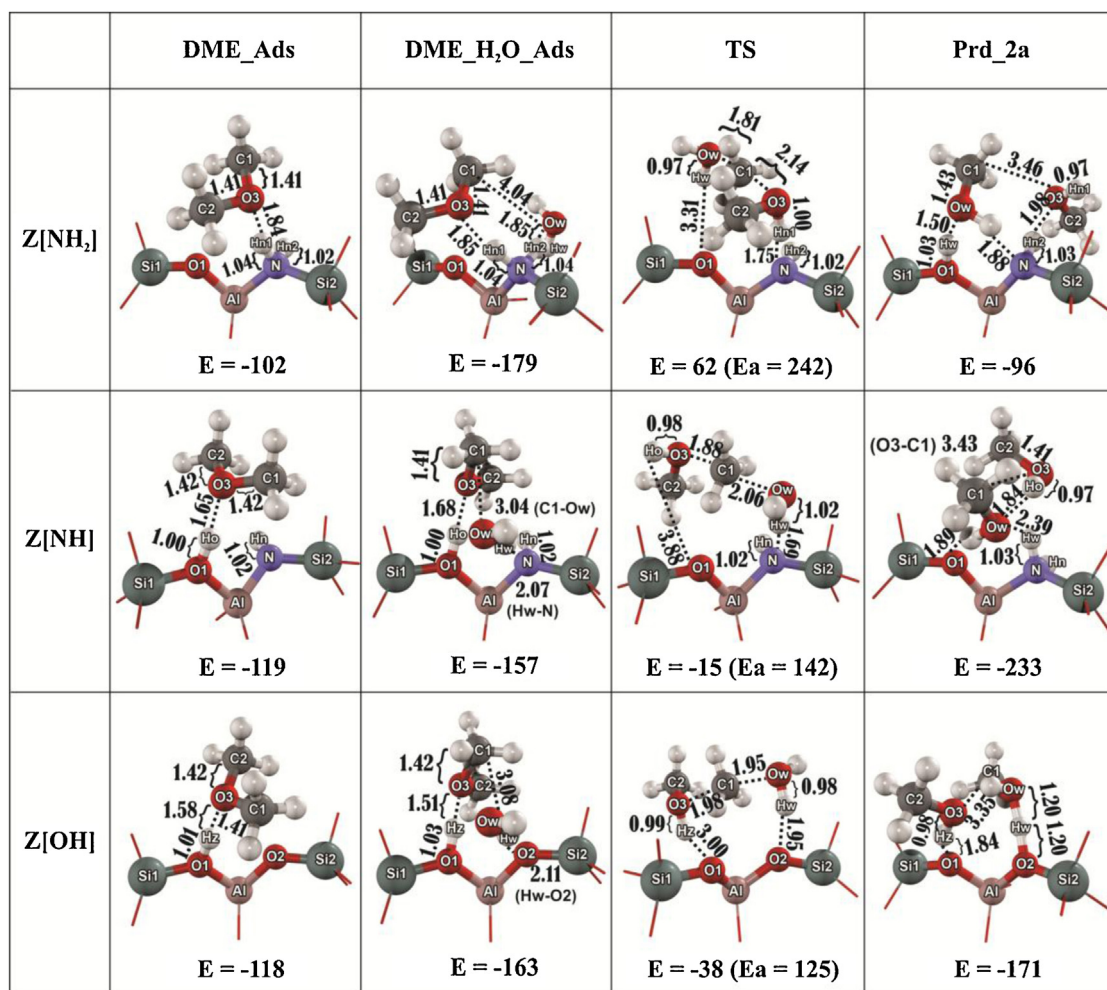
Fig. 3. Optimized structures of all stationary points for the DME hydrolysis step of the concerted mechanism of the DME hydrolysis over the Z[NH$_2$], Z[NH] and Z[OH]. Energies (E) are in kJ/mol and distances are in Å.

concerted reaction are more kinetically preferred over the Z[OH] and it is decreased in the sequences of the order; Z[OH] > Z[NH] > Z[NH$_2$].

B. Stepwise channel: The stepwise channel also consists of two steps namely (1) the demethylation and (2) the hydrolysis.

(B1) The demethylation step: Fig. 6 shows the optimized structures of stationary points along this step and Tables S4, S5, and S6 (see supporting information) list the selected parameters for all complexes of the demethylation in the Z[NH$_2$], Z[NH] and Z[OH] centers, respectively. This step starts with the adsorption of DME on Brønsted acid site to form the DME adsorption complexes (DME_Ads). These complexes proceed to the intermediates (denoted as Int_1) via the first transition states (denoted as TS_1). At the TS_1 structures, the C1-O3 bonds are breaking and the O3—Hz bonds (O3—Ho, O3—Hn1) are forming simultaneously. Then, the first product methanol is formed binding to the methyl-surface intermediate (denoted as Int_1). It is noted that the methyl-surface intermediate for the Z[NH] model is the methylammonium complex (CH$_3$-NH-Z) whereas those for the others are the methoxide complexes (CH$_3$—O—Z). The three TS_1 structures were confirmed by normal mode analyses that each structure has one imaginary frequency (405i cm^{-1} for Z[OH], 454i cm^{-1} for Z[NH] and 395i cm^{-1} for Z[NH$_2$]) corresponding to the reaction coordinate described above. For this step, the calculated barriers ($E_{TS}1$) referenced to the separated reactants are 76, 63 and 169 kJ/mol while the intrinsic barriers (E_a1) are 194, 181 and 271 kJ/mol, for the Z[OH], Z[NH],

and Z[NH$_2$] centers, respectively. The results suggest that the Z[NH] has the highest reactivity for the first methanol Int_1 formation. This also confirms previous reports showing that the Z[NH] highly activated the alkylammonium formations from methylation [19], and ethylation [22]. It is worth to note that the activation barriers for the Z[NH$_2$] are greater than those for the Z[NH] and the Z[OH] due to its acidic proton (Hn1) has the lowest acidity as mentioned earlier. Thus, the formation of the alkoxide is not possible at Z[NH$_2$] site. This agrees with the report from Lesthaeghe et al. [20].

The adsorbed product methanol in the Int_1 complexes can desorb to form the stable methoxide (CH$_3$-O-Z) or methylammonium (CH$_3$-NH-Z) species with energies of 54, −64 and 109 kJ/mol (relative to separated reactants) for the Z[OH], Z[NH], and Z[NH$_2$] centers, respectively. It can be explained that due to nitrogen atom has a stronger lewis basicity compared to oxygen atom, therefore the covalent N-C bond of the Z[NH] is stronger than the O—C bonds of the Z[OH] and Z[NH$_2$]. These observations are consistent to the previous studies of Lesthaeghe et al. [19] and Zheng et al. [22] where they predicted that the Z[NH] is a potential catalysts for the acid/base functional reaction compared to the undoped H-ZSM-5. However, as indicated earlier, the alkyl-surface species is not a final product for any reactions catalyzed by zeolites but it is an intermediate that must be further converted to the desired product by the hydrolysis step as described below.

(B2) The hydrolysis step: The optimized structures for the hydrolysis of the methyl surface species Int_2 to produce the second
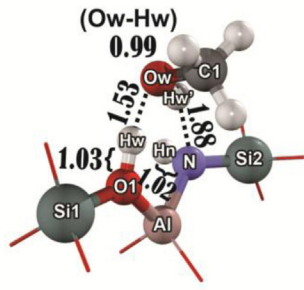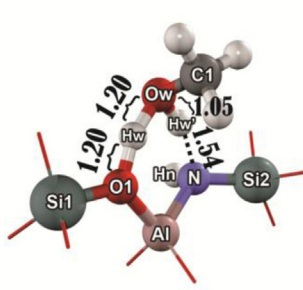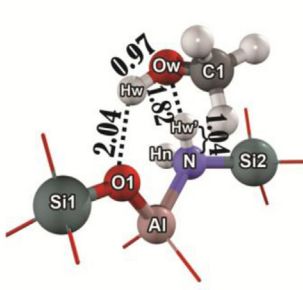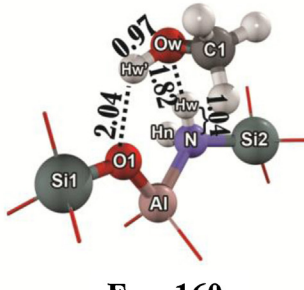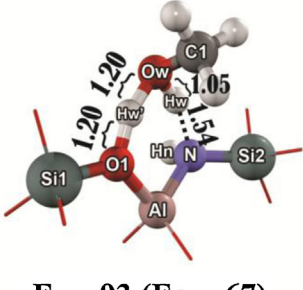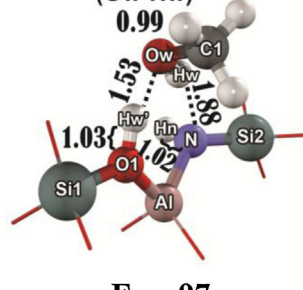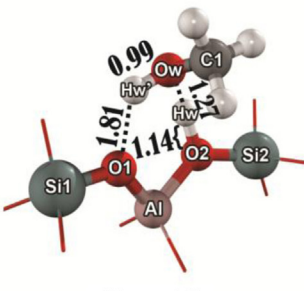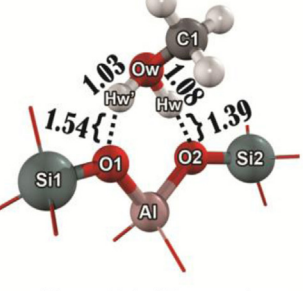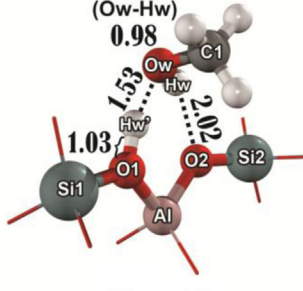
Fig. 4. Optimized structures of all stationary points for the proton shuttle step of the concerted mechanism of the DME hydrolysis over the Z[NH$_2$], Z[NH] and Z[OH]. Energies (E) are in kJ/mol and distances are in Å.

methanol over the three active sites are depicted in Fig. 7 and the selected parameters are listed in Tables S7, S8 and S9 (see supporting information). In this step, the reaction proceeds when the water molecule adsorbs next to the methyl-surface species (Int_2) to form the methoxide–water or methylammonium–water co-adsorption complex (denoted as Co_Ads). The relative energies of the Co_Ads respected to the associated Int_2 are equivalent to the interaction of water with the Int_2 and are calculated to be −14, −143 and 55 kJ/mol for the Z[OH], Z[NH] and Z[NH$_2$], respectively. The hydrolysis step proceeds via transition states (TS_2) generated by a bond forming between the water oxygen (Ow) and the methyl C1 (the Ow–C1 bond distances are 1.89, 1.75, and 1.89 Å at Z[OH], Z[NH] and Z[NH$_2$] center, respectively) simultaneously with the breaking of the C1–O2 bond at Z[OH] (2.16 Å), the C1–N bond at Z[NH] (2.46 Å) and the C1–O1 bond at Z[NH$_2$] (2.23 Å). The

hydrogen water (Hw) is transferred to oxygen atom of zeolite to regenerate the Brønsted acid site. Normal mode analyses reveal that these TS's each has one major imaginary frequency that has the value of 341i, 341i and 328i cm^{-1} for the Z[OH], Z[NH] and Z[NH$_2$], respectively corresponding to the reaction motion. The product of the reaction (Prd_1s) is formed as methanol side-on adsorbed on the acid site with one hydrogen bonding between the oxygen of methanol (Ow) and the proton of zeolite (Hw) (see Fig. 7). This complex can easily transform to more stable end-on structure (Prd_1e) as found for the concerted channel. The adsorbed methanol is finally desorbed from the acid site to regenerate the active center.

The apparent activation energies for the hydrolysis step ($E_{TS}2$) are calculated to be 99, 85 and 193 kJ/mol while the intrinsic activation energies (E_a2) are 112, 228 and 139 kJ/mol, for the Z[OH], Z[NH] and Z[NH$_2$], respectively. Note that hydrolysis over a Z[NH] center
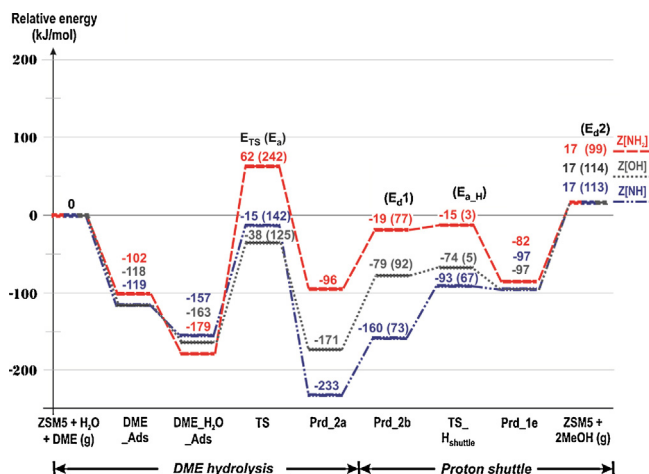
Fig. 5. Comparison of the energy profiles for the concerted mechanism of the DME hydrolysis over Z[OH], Z[NH], and Z[NH$_2$] calculated by ONIOM method. Energies are in kJ/mol. E_{TS} = apparent activation energy of the DME hydrolysis, E_a = intrinsic activation energy of the DME hydrolysis ($E_{TS} - E_{DME.H2O\_Ads}$), $E_{a.H}$ = intrinsic activation energy of the proton shuttle, E_d1 = desorption energy of the first methanol, E_d2 = desorption energy the second methanol.

has the highest intrinsic activation barrier of 228 kJ/mol (relative to the methylammonium surface species) to convert methylammonium to methanol but has the lowest apparent activation energy (relative to separated reactants) since this surface intermediate is quite stable. Due to its stability, the methylammonium species could also be precursors for coke formation in the Z[NH] catalyst. This finding clearly indicates that the amine-doped zeolite may not be a good catalyst for hydrocarbon conversions that proceed via alkyl-surface intermediate since these intermediates are too stable to regenerate the catalytic center.

For the stepwise channel, Fig. 8 shows that the activation barrier of the hydrolysis step (E_a2 = 112 kJ/mol) in the Z[OH] is much lower than that of the demethylation step (E_a1 = 194 kJ/mol). This result is consistent with the experimental observation reported that the hydrolysis of surface-alkoxide species to alcohol over zeolite occurs rapidly [21]. The apparent activation barrier of the entire reaction in the Z[OH], calculated to be 99 kJ/mol (black dot line), is comparable to the Arrhenius activation energy of 76.5 kJ/mol reported in our previous study [4].

3.4. Comparison between the stepwise and concerted channels

Comparing energy profiles for both reaction channels in Figs. 5 and 8 shows that in all three catalytic centers the energy profile along the concerted channel is lower than that of the stepwise
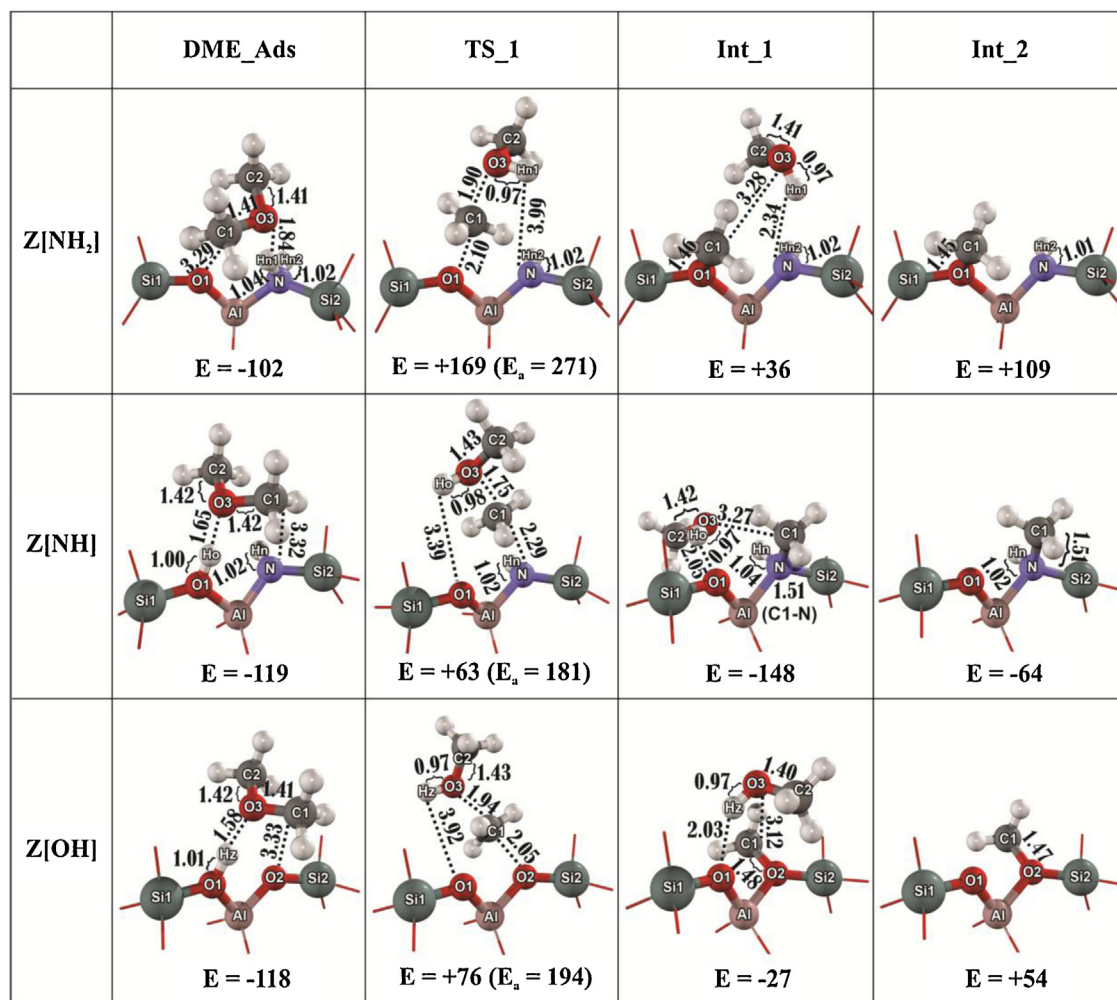

Fig. 6. Optimized structures of all stationary points for the demethylation step (first step) of the stepwise mechanism of the DME hydrolysis over the Z[NH$_2$], Z[NH] and Z[OH]. Energies (E) are in kJ/mol and distances are in Å.
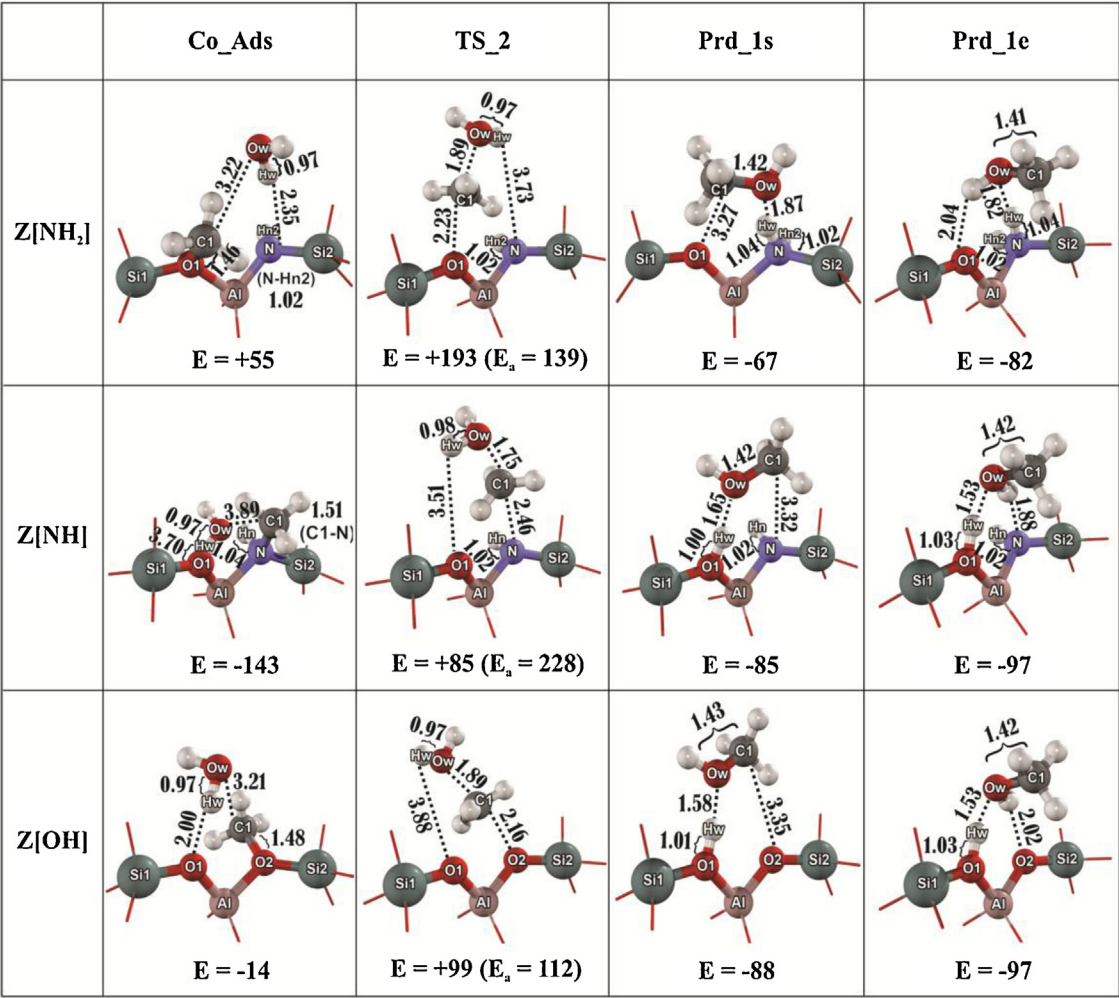
Fig. 7. Optimized structures of all stationary points for the hydrolysis step (second step) of the stepwise mechanism of the DME hydrolysis over the Z[NH$_2$], Z[NH] and Z[OH]. Energies (E) are in kJ/mol and distances are in Å.
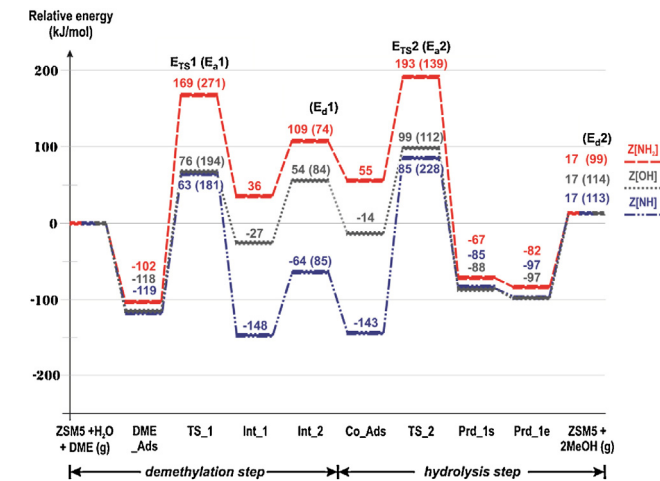

Fig. 8. Comparison of the energy profiles for the stepwise mechanism of the DME hydrolysis over Z[OH], Z[NH] and Z[NH$_2$] calculated by the ONIOM method. Energies are in kJ/mol. $E_{TS}1$ = first apparent activation energy. E_a1 = first intrinsic activation energy ($E_{TS}1 - E_{DME\_Ads}$). $E_{TS}2$ = second apparent activation energy. E_a2 = second intrinsic activation energy ($E_{TS}2 - E_{Co\_Ads}$). E_d = desorption energy of methanol.

channel. These indicate that the DME hydrolysis over the three active centers favor the concerted mechanism. Fig. 5 shows that the activation barriers of the rate-determining step for the concerted mechanism calculated to be 125, 142 and 242 kJ/mol for the Z[OH], Z[NH] and Z[NH$_2$] centers, respectively, predict the trend of catalytic reactivity of the three models as in the order, Z[OH] > Z[NH] > Z[NH$_2$].

3.5. Effect of QM size in ONIOM2 scheme

To confirm that our ONIOM2 cluster model have provided accurate results, we tested the calculations by extending the size of QM region from 12T to 23T by connecting the 12T with the 11T as shown in Fig. 9. This 23T region is similar to the 22T QM cluster that has been employed to simulate the active site of H-ZSM-5 zeolite for study some hydrocarbon reactions such as isomerization [47] and dehydration [48]. In this section, to study the effect of the QM sizes, the mechanism of DME hydrolysis on normal Brønsted acid Z[OH] site has been investigated by comparing the results obtained from the new 23T:128T and 12T:128T ONIOM2 models. The calculated energies of all complexes are shown in Figs. S1 and S2 while the geometrical parameters are listed in Table S4–S7. These calculated results are obtained by the same conditions for the two models. We found that the increasing of QM size is not significant to the results in terms of structures and energies. The geometrical parameters
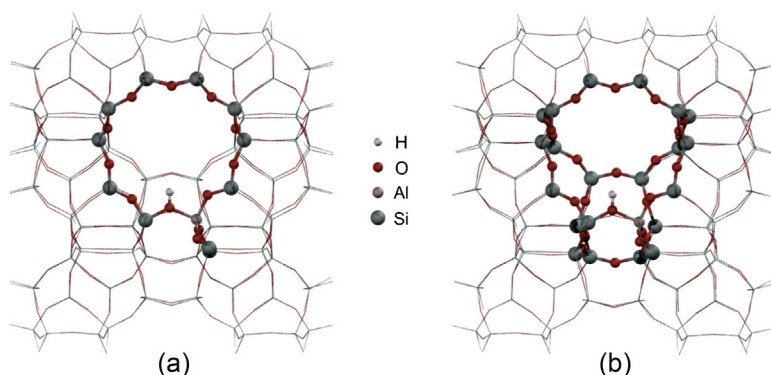
Fig. 9. The 128T cluster of H-ZSM-5 zeolite modeled by the ONIOM2 (M06/6-31G(d,p):UFF). The quantum region is represented by balls and sticks while the UFF is drawn as lines: (a) 12T quantum region and (b) 23T quantum region.

that obtained from 23T QM size are quite similar to that of the 12T QM. The energy differences for reactants, intermediates and products obtained from the two models are almost equivalent (with in 3 kJ/mol). In the case of transition state structures, however, the energies of the 23T:128T cluster is lower than that of the 12T:128T cluster by about 10 kJ/mol. Nevertheless, the differences in energies are rather small while the trend of energy profiles in the both of concerted and stepwise pathways are unchanged. Therefore, we have confidence that the 12T:128T ONIOM2 model is sufficient for study this reaction.

4. Conclusion

In this computational study, the embedded cluster ONIOM method was employed to investigate the effects of doping amine to ZSM-5 on its catalytic activity for hydrolysis of DME to methanol. Amine-doped ZSM-5 has three active centers namely the Brønsted acid site Z[OH] and the two new Z[NH$_2$], and Z[NH] active sites. The reaction has two possible stepwise and concerted channels. The stepwise channel starts with the demethylation step to produce the first methanol and the methyl-surface intermediate. The produced intermediates for the Z[OH] and Z[NH$_2$] models are the methoxide while that for the Z[NH] is the methylammonium. The second step is the hydrolysis of the intermediate to the second methanol. The intrinsic activation energies of the demethylation step are 194, 181 and 271 kJ/mol and those of the hydrolysis step are 112, 228 and 139 kJ/mol for the Z[OH], Z[NH] and Z[NH$_2$], respectively. The rate-limiting step for the Z[OH] and Z[NH$_2$] is the demethylation while that for the Z[NH] is the hydrolysis step. Alternatively, the concerted channel consists of DME hydrolysis and proton shuttle steps where the first step is the rate-determining step. We predicted that the DME favor to be hydrolyzed to methanol via concerted channel for the three active centers because their activation barriers of the rate-determining step which are calculated to be 125, 142 and 242 kJ/mol for the Z[OH], Z[NH] and Z[NH$_2$], respectively, are lower than those of the rate-determining step of the stepwise channel. Our calculations demonstrate the usefulness of computational chemistry in catalytic investigation of the designed catalysts. The results show that the amine-doped ZSM-5 in the non-protonated form (Z[NH]) can activate the methylammonium formation, while the following process to final product requires extremely high energy compared to undoped ZSM-5.

Acknowledgements

Appendix A. Supplementary data

Supplementary data associated with this article can be found, in the online version, at http://dx.doi.org/10.1016/j.jmgm.2013.03.006.

References

[1] T.A. Semelsberger, R.L. Borup, H.L. Greene, Dimethyl ether (DME) as an alternative fuel, Journal of Power Sources 156 (2006) 497–511.
[2] K. Takeishi, H. Suzuki, Steam reforming of dimethyl ether, Applied Catalysis A: General 260 (2004) 111–117.
[3] K. Faungnawakij, Y. Tanaka, N. Shimoda, T. Fukunaga, S. Kawashima, R. Kikuchi, K. Eguchi, Influence of solid-acid catalysts on steam reforming and hydrolysis of dimethyl ether for hydrogen production, Applied Catalysis A: General 304 (2006) 40–48.
[4] S. Namuangruk, J. Meeprasert, P. Khemthong, K. Faungnawakij, A combined experimental and theoretical study on the hydrolysis of dimethyl ether over H-ZSM-5, Journal of Physical Chemistry C 115 (2011) 11649–11656.
[5] K. Faungnawakij, R. kikuchi, T. Matsui, T. Fukunaga, K. Eguchi, A comparative study of solid acids in hydrolysis and steam reforming of dimethyl ether, Applied Catalysis A: General 333 (2007) 114–121.
[6] T.A. Semelsberger, K.C. Ott, R.L. Borup, H.L. Greene, Role of acidity on the hydrolysis of dimethyl ether (DME) to methanol, Applied Catalysis B: Environmental 61 (2005) 281–287.
[7] S.R. Blaszkowski, R.A. van Santen, The mechanism of dimethyl ether formation from methanol catalyzed by zeolitic protons, Journal of the American Chemical Society 118 (1996) 5152.
[8] S.R. Blaszkowski, R.A. van Santen, Theoretical study of the mechanism of surface methoxy and dimethyl ether formation from methanol catalyzed by zeolite protons, Journal of Physical Chemistry B 101 (1997) 2292–2305.
[9] T. Maihom, B. Boekfa, J. sirijaraensre, T. Nanok, M. Probst, J. Limtrakul, Reaction mechanism of methylation of ethene with methanol and dimethyl ether over H-ZSM-5: an ONIOM study, Journal of Physical Chemistry C 113 (2009) 6654–6662.
[10] K. Yamamoto, Y. Sakata, Y. Nohara, Y. Takahashi, T. Tatsumi, Organic–inorganic hybrid zeolites containing organic frameworks, Science 300 (2003) 470–472.
[11] D. Lesthaeghe, G. Delcour, V.V. Speybroeck, G.B. Marin, M. Waroquier, Theoretical study on the alteration of fundamental zeolite properties by methylene functionalization, Microporous and Mesoporous Materials 96 (2006) 350–356.
[12] K.D. Hammond, F. Dogan, G.A. Tompsett, V. Agarwal, W.C. Conner, C.P. Gray, S.M. Auerbach, Spectroscopic signatures of nitrogen-substituted zeolites, Journal of the American Chemical Society 130 (2008) 14912–14913.
[13] G. Wu, X. Wang, Y. Yang, L. Li, G. Wang, N. Guan, Confirmation of NH species in the framework of nitrogen-incorporated ZSM-5 zeolite by experimental and theoretical studies, Microporous and Mesoporous Materials 127 (2010) 25–31.
[14] V. Agarwal, G.W. Huber, W.C. Conner, S.M. Auerbach, DFT study of nitrided zeolites: mechanism of nitrogen substitution in HY and silicalite, Journal of Catalysis 269 (2010) 53–63.
[15] R. Astala, S.M. Auerbach, The properties of methylene- and amine-substituted zeolites from first principles, Journal of the American Chemical Society 126 (2003) 1843–1848.
[16] G.J. Wu, N.J. Guan, L.D. Li, Recent development of nitrogen-incorporated molecular sieves, Chinese Journal of Catalysis 33 (2012) 51–59.

[17] M. Elanany, B.-L. Su, D.P. Vercauteren, The effect of framework organic moieties on the acidity of zeolites: a DFT study, Journal of Molecular Catalysis A 263 (2007) 195–199.

[18] K. Hemelsoet, D. Lesthaeghe, V.V. Speybroeck, M. Waroquier, Bifunctional acid-base catalyzed reactions in zeolites from the HSAB viewpoint, Chemical Physics Letters 419 (2006) 10–15.

[19] D. Lesthaeghe, V.V. Speybroeck, G.B. Marin, M. Waroquier, DFT investigated of alkoxide vs alkylammonium formation in amine-substituted zeolites, Journal of Physical Chemistry B 109 (2005) 7952–7960.

[20] D. Lesthaeghe, V. Van Speybroeck, M. Waroquier, Efficient use of bifunctional acid–base properties for alkylammonium formation in amine-substituted zeolites, Journal of the American Chemical Society 126 (2004) 9162–9163.

[21] W. Wang, M. Hunger, Reactivity of surface alkoxy on acidic zeolites, Accounts of Chemical Research 41 (2008) 895–904.

[22] A. Zheng, L. Wang, L. Chen, Y. You, C. Ye, X. Lu, F. Deng, High activity of amine-doped H-ZSM-5 zeolite in ethene protonation: revealed by embedding calculations, ChemPhysChem 8 (2007) 231–234.

[23] M. Svensson, S. Humbel, R.D.J. Froese, T. Matsubara, S. Sieber, K. Morokuma, Journal of Physical and Chemical 100 (1996) 19357.

[24] S. Namuangruk, P. Khongpracha, P. Pantu, J. Limtrakul, Journal of Physical Chemistry B 110 (2006) 25950–25957.

[25] S. Namuangruk, P. Pantu, J. Limtrakul, Journal of Catalysis 225 (2004) 523–530.

[26] S. Namuangruk, P. Pantu, J. Limtrakul, ChemPhysChem 6 (2005) 1333–1339.

[27] Y.-X. Sun, J. Yang, L.-F. Zhao, J.-X. Dai, H. Sun, Journal of Physical Chemistry C 114 (2010) 5975–5984.

[28] H. van Koningsveld, H. van Bekkum, J.C. Jansen, On the location and disorder of the tetrapropylammonium (TPA) ion in zeolite ZSM-5 with improved framework accuracy, Acta Crystallographica B43 (1987) 127–132.

[29] T. Baba, N. Komatsu, Y. Ono, Mobility of the acidic protons in H-ZSM-5 as studied by variable temperature 1H MAS NMR, Journal of Physical Chemistry B 102 (1998) 804–808.

[30] X. Guan, N. Li, G. Wu, J. Chen, F. Zhang, N. Guan, Para-selectivity of modified HZSM-5 zeolites by nitridation for ethylation of ethylbenzene with ethanol, Journal of Molecular Catalysis A 248 (2006) 220–225.

[31] P. Sarv, T. Tuherm, E. Lippmaa, K. Keskinen, A. Root, Mobility of the acidic proton in bronsted sites of H-Y, H-Mordenite, and H-ZSM-5 zeolites, studied by high-temperature 1H MAS NMR, Journal of Physical Chemistry 99 (1995) 13763–13768.

[32] J. Sirijaraensre, J. Limtrakul Structures and mechanisms of the dehydration of benzaldoxime over Fe-ZSM-5 zeolites: a DFT study, Struct. Chem. DOI 10.1007/s11224-012-0161, 1–12.

[33] M.J. Frisch, G.W. Trucks, H.B. Schlegel, G.E. Scuseria, M.A. Robb, J.R. Cheeseman, J.A. Montgomery, Jr., T. Vreven, K.N. Kudin, J.C. Burant, J.M. Millam, S.S. Iyengar, J. Tomasi, V. Barone, B. Mennucci, M. Cossi, G. Scalmani, N. Rega, G.A. Petersson, H. Nakatsuji, M. Hada, M. Ehara, K. Toyota, R. Fukuda, J. Hasegawa, M. Ishida, T. Nakajima, Y. Honda, O. Kitao, H. Nakai, M. Klene, X. Li, J.E. Knox, H.P. Hratchian, J.B. Cross, C. Adamo, J. Jaramillo, R. Gomperts, R.E. Stratmann, O. Yazyev, A.J. Austin, R. Cammi, C. Pomelli, J.W. Ochterski, P.Y. Ayala, K. Morokuma, G.A. Voth, P. Salvador, J.J. Dannenberg, V.G. Zakrzewski, S. Dapprich, A.D. Daniels, M.C. Strain, O. Farkas, D.K. Malick, A.D. Rabuck, K. Raghavachari, J.B. Foresman, J.V. Ortiz, Q. Cui, A.G. Baboul, S. Clifford, J. Cioslowski, B.B. Stefanov, G. Liu, A. Liashenko, P. Piskorz, I. Komaromi, R.L. Martin, D.J. Fox, T. Keith, M.A. Al-Laham, C.Y. Peng, A. Nanayakkara, M. Challacombe, P.M.W. Gill, B. Johnson, W. Chen, M.W. Wong, C. Gonzalez, and J.A. Pople, Gaussian 03, Pittsburgh, PA, 2003.

[34] J. Datka, M. Boczar, P. Rymarowicz, Heterogeneity of OH groups in NaH-ZSM-5 zeolite studied by infrared spectroscopy, Journal of Catalysis 114 (1988) 368–376.

[35] M.A. Makarova, K.M. Al-Ghefaili, J. Dwyer, Bronsted acid strength in US-Y: FTIR study of CO adsorption, Journal of the Chemical Society-Faraday Transactions. 90 (1994) 383–386.

[36] U. Eichler, M. Brandle, J. Sauer, Predicting absolute and site specific acidities for zeolite catalysts by a combined quantum mechanics/interatomic potential function approach, Journal of Physical Chemistry B 101 (1997) 10035–10050.

[37] K. Sillar, P. Burk, Calculation of the properties of acid sites of the zeolite ZSM-5 using ONIOM method, Journal of Molecular Structure (Theochem) 589–590 (2002) 281–290.

[38] C.C. Lee, R.J. Gorte, W.E. Farneth, Calorimetric study of alcohol and nitrile adsorption complexes in H-ZSM-5, The Journal of Physical Chemistry B 101 (1997) 3811–3817.

[39] J. Andzelm, N. Govind, G. Fitzgerald, A. Maiti, DFT study of methanol conversion to hydrocarbons in a zeolite catalyst, International Journal of Quantum Chemistry 91 (2003) 467–473.

[40] A.M. Vos, K.H.L. Nulens, F. De Proft, R.A. Schoonheydt, P. Geerlings, Reactivity descriptors and rate constants for electrophilic aromatic substitution:‰ acid zeolite catalyzed methylation of benzene and toluene, The Journal of Physical Chemistry B 106 (2002) 2026–2034.

[41] B. Jansang, T. Nanok, J. Limtrakul, Structure and reaction mechanism of alkylation of phenol with methanol over H-FAU zeolite: an ONIOM study, The Journal of Physical Chemistry C 112 (2007) 540–547.

[42] S.R. Blaszkowski, R.A. van Santen, Density functional theory calculations of the activation of methanol by a Broensted zeolitic proton, The Journal of Physical Chemistry 99 (1995) 11728–11738.

[43] S.R. Blaszkowski, R.A. van Santen, The mechanism of dimethyl ether formation from methanol catalyzed by zeolitic protons, Journal of the American Chemical Society 118 (1996) 5152–5153.

[44] C.-C. Lee, R.J. Gorte, Calorimetric study of alcohol and nitrile adsorption complexes in H-ZSM-5, Journal of Physical Chemistry B 101 (1997) 3811–3817.

[45] T. Fujino, M. Kashitani, J.N. Kondo, K. Domen, C. Hirose, M. Ishida, F. Goto, F. wakabayashi, FT-IR and quantum chemical studies of interaction between dimethyl ether and HZSM-5 zeolite, Journal of Physical Chemistry 100 (1996) 11649–11653.

[46] A. Zheng, L. Wang, L. Chen, Y. You, C. Ye, X. Lu, F. Deng, Prediction of the 13C NMR chemical shifts of organic species adsorbed on H-ZSM-5 zeolite by the ONIOM-GIAO method, Chemical Communications (2005) 2474–2476.

[47] G. Barone, N. Armata, A. Prestianni, T. Rubino, D. Duca, D.Y. Murzin, Confined But-2-ene catalytic isomerization inside H-ZSM-5 Models: a DFT study, Journal of Chemical Theory and Computation 5 (2009) 1274–1283.

[48] A. Prestianni, R. Cortese, D. Duca, Propan-2-ol dehydration on H-ZSM-5 and H-Y zeolite: a DFT study, reaction kinetics, Mechanisms and Catalysis 108 (2013) 565–582.